

# Deep Learning for Mean Field Games with non-separable Hamiltonians

Mouhcine Assouli<sup>a</sup>, Badr Missaoui<sup>b</sup>

<sup>a</sup>*Modeling, Simulation and Data Analysis Lab, Lot 660, Ben Guerir, 43150, Morocco*

<sup>b</sup>*Modeling, Simulation and Data Analysis Lab, Lot 660, Ben Guerir, 43150, Morocco*

---

## Abstract

This paper introduces a new method based on Deep Galerkin Methods (DGMs) for solving high-dimensional stochastic Mean Field Games (MFGs). We achieve this by using two neural networks to approximate the unknown solutions of the MFG system and forward-backward conditions. Our method is efficient, even with a small number of iterations, and is capable of handling up to 300 dimensions with a single layer, which makes it faster than other approaches. In contrast, methods based on Generative Adversarial Networks (GANs) cannot solve MFGs with non-separable Hamiltonians. We demonstrate the effectiveness of our approach by applying it to a traffic flow problem, which was previously solved using the Newton iteration method only in the deterministic case. We compare the results of our method to analytical solutions and previous approaches, showing its efficiency. We also prove the convergence of our neural network approximation with a single hidden layer using the universal approximation theorem.

*Keywords:* Mean Field Games, Deep Learning, Deep Galerkin Method, Traffic Flow, Non-Separable Hamiltonian

---

## 1. Introduction

Mean Field Games (MFGs) are a widely studied topic that can model a variety of phenomena, including autonomous vehicles [1, 2], finance [3, 4], economics [5, 6, 7], industrial engineering [8, 9, 10], and data science [11, 12]. MFGs are dynamic, symmetric games where the agents are indistinguishable but rational, meaning that their actions can affect the mean of the population. In the optimal case, the MFG system reaches a Nash equilibrium

(NE), in which no agent can further improve their objective. MFGs are described by a system of coupled partial differential equations (PDEs) known as equation

$$\begin{cases} -\partial_t \phi - \nu \Delta \phi + H(x, \rho, \nabla \phi) = 0, & \text{in } E_1, \\ \partial_t \rho - \nu \Delta \rho - \operatorname{div}(\rho \nabla_p H(x, \rho, \nabla \phi)) = 0, & \text{in } E_2, \\ \rho(0, x) = \rho_0(x), \quad \phi(T, x) = g(x, \rho(T, x)), & \text{in } \Omega, \end{cases} \quad (1)$$

where,  $E_1 = (0, T] \times \Omega$ ,  $E_2 = [0, T) \times \Omega$ ,  $\Omega \subset \mathbb{R}^d$  and  $g$  denotes the terminal cost. The Hamiltonian  $H$  with separable structure is defined as

$$H(x, \rho, p) = \inf_v \{-p \cdot v + L_0(x, v)\} - f_0(x, \rho) = H_0(x, p) - f_0(x, \rho), \quad (2)$$

consisting of a forward-time Fokker-Planck equation (FP) and a backward-time Hamilton-Jacobi-Bellman equation (HJB), which describe the evolution of the population density ( $\rho$ ) and the cost value ( $\phi$ ), respectively. The PDEs are defined in the domain  $E_1 = (0, T] \times \Omega$  and  $E_2 = [0, T)$ . The Hamiltonian  $H$  has a separable structure and is defined as the infimum of the Lagrangian function  $L_0$ , which is the Legendre transform of the Hamiltonian, minus the interaction function  $f_0$  between the population of agents. The MFG system also includes boundary conditions, with the initial density  $\rho(0, x)$  given by  $\rho_0(x)$  and the terminal cost  $\phi(T, x)$  given by  $g(x, \rho(T, x))$ . These boundary conditions apply in the domain  $\Omega \subset \mathbb{R}^d$ .

One of the main challenges of MFGs is the viscosity problem, in addition to the complexity of the PDEs and forward-backward conditions. Many methods for solving MFGs are limited to the deterministic setting ( $\nu = 0$ ). For example, the Newton iteration method has been applied to the problem of traffic flow in [1], where a flexible machine learning framework was provided for the numerical solution of potential MFGs. While numerical methods do exist for solving the system of PDEs (1) [13, 14, 15, 16], they are not always effective due to computational complexity, especially in high dimensional problems. Deep learning methods, such as Generative Adversarial Networks (GANs) [17, 18], have been used to address this issue by reformulating MFGs as a primal-dual problem [19, 20, 14]. This approach uses the Hopf formula in density space [21] to establish a connection between MFGs and GANs. However, this method requires the Hamiltonian  $H$  to be separable in  $\rho$  and  $p$ . In cases where the Hamiltonian is non-separable, such as in traffic flow [1], it is not possible to reformulate MFGs as a primal-dual

problem. Recently, [22] proposed a policy iteration algorithm for MFGs with non-separable Hamiltonians using the contraction fixed point method.

*Contributions* In this work, we present a new method based on DGM for solving stochastic MFG with a non-separable Hamiltonian. Inspired by the work [23, 24, 25], we approximate the unknown solutions of the system (1) by two neural networks trained simultaneously to satisfy each equation of the MFGs system and forward-backward conditions. While the GAN-based techniques are limited to problems with separable Hamiltonians, our algorithm, called New-Method, can solve any MFG system. Moreover, we prove the convergence of the neural network approximation with a single layer using a fundamental result of the universal approximation theorem. Then, we test the effectiveness of our New-Method through several numerical experiments, where we compare our results of New-Method with previous approaches to assess their reliability. At last, our approach is applied to solve the MFG system of traffic flow accounting for the stochastic case.

*Contents* The structure of the rest of the paper is as follows: in Section 2, we introduce the main description of our approach. Section 3 examines the convergence of our neural network approximation with a single hidden layer. In Section 4, we present a review of prior methods. Section 5 investigates the numerical performance of our proposed algorithms. We evaluate our method using a simple analytical solution in Section 5.1 and compare it to the previous approach in Section 5.2. We also apply our method to the traffic flow problem in Section 5.3. Finally, we conclude the paper and discuss potential future work in Section 6.

## 2. Methodology

Our method involves using two neural networks,  $N_\theta$  and  $N_\omega$ , to approximate the unknown variables  $\rho$  and  $\phi$ , respectively. The weights for these networks are  $\theta$  and  $\omega$ . Each iteration of our method involves updating  $\rho$  and  $\phi$  with the approximations from  $N_\theta$  and  $N_\omega$ . To optimize the accuracy of these approximations, we use a loss function based on the residual of the first equation (HJB) to update the parameters of the neural networks. We repeat this process using the second equation (FP) and new parameters; see Figure 1. Both neural networks are simultaneously trained on the first equation, and the results are then checked in the second equation, where they are

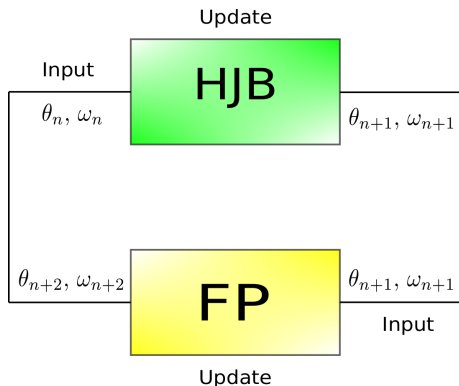


Figure 1: The learning mechanism of our method.

fine-tuned until an equilibrium is reached. This equilibrium represents the convergence of the two neural networks and, therefore, the solution to both the Hamilton Jacobi Bellman equations and the Fokker-Planck equation.

We have developed a solution for the problem of MFG systems 1 that does not rely on the Hamiltonian structure. Our approach involves using a combination of physics-informed deep learning [24] and deep hidden physics models [25] to train our model to solve high-dimensional PDEs that adhere to specified differential operators, initial conditions, and boundary conditions. Our model is also designed to adhere to general nonlinear partial differential equations that describe physical laws. To train our model, we define a loss function that minimizes the residual of the equation at randomly chosen points in time and space within the domain  $\Omega$ .

We initialize the neural networks as a solution to our system. We let:

$$\phi_\omega(t, x) = N_\omega(t, x), \quad \rho_\theta(t, x) = N_\theta(t, x). \quad (3)$$

Our training strategy starts by solving (HJB). We compute the loss (4) at randomly sampled points  $\{(t_{b_1}, x_{b_1})\}_{b_1=1}^{B_1}$  from  $E_1$ , and  $\{x_{s_1}\}_{s_1=1}^{S_1}$  from  $\Omega$ .

$$\text{LOSS}_{total}^{(HJB)} = \text{LOSS}^{(HJB)} + \text{LOSS}_{cond}^{(HJB)}, \quad (4)$$

where

$$\begin{aligned} \text{LOSS}^{(HJB)} = \frac{1}{B_1} \sum_{b_1=1}^{B_1} & \left| \partial_t \phi_\omega(t_{b_1}, x_{b_1}) + \nu \Delta \phi_\omega(t_{b_1}, x_{b_1}) \right. \\ & \left. - H(x_{b_1}, \rho_\theta(t_{b_1}, x_{b_1}), \nabla \phi_\omega(t_{b_1}, x_{b_1})) \right|^2, \end{aligned}$$

and

$$\text{LOSS}_{cond}^{(HJB)} = \frac{1}{S_1} \sum_{s_1=1}^{S_1} \left| \phi_\omega(T, x_{s_1}) - g(x_{s_1}, \rho_\theta(T, x_{s_1})) \right|^2.$$

We then update the weights of  $\phi_\omega$  and  $\rho_\theta$  by back-propagating the loss (4). We do the same to (FP) with the updated weights. We compute (5) at randomly sampled points  $\{(t_{b_2}, x_{b_2})\}_{b_2=1}^{B_2}$  from  $E_2$ , and  $\{x_{s_2}\}_{s_2=1}^{S_2}$  from  $\Omega$ .

$$\text{LOSS}_{total}^{(FP)} = \text{LOSS}^{(FP)} + \text{LOSS}_{cond}^{(FP)}, \quad (5)$$

where

$$\begin{aligned} \text{LOSS}^{(FP)} = \frac{1}{B_2} \sum_{b_2=1}^{B_2} & \left| \partial_t \rho_\theta(t_{b_2}, x_{b_2}) - \nu \Delta \rho_\theta(t_{b_2}, x_{b_2}) \right. \\ & \left. - \text{div}(\rho_\theta(t_{b_2}, x_{b_2}) \nabla_p H(x_{b_2}, \rho_\theta(t_{b_2}, x_{b_2}), \nabla \phi_\omega(t_{b_2}, x_{b_2}))) \right|^2, \end{aligned}$$

and

$$\text{LOSS}_{cond}^{(FP)} = \frac{1}{S_2} \sum_{s_2=1}^{S_2} \left| \rho_\theta(0, x_{s_2}) - \rho_0(x_{s_2}) \right|^2.$$

Finally, we update the weights of  $\phi_\omega$  and  $\rho_\theta$  by back-propagating the loss (5); see Algorithm [1].

### 3. Convergence

Following the steps of [23], this section presents theoretical results that guarantee the existence of a single layer feedforward neural networks  $\rho_\theta$  and  $\phi_\omega$  which can universally approximate the solutions of (1). Denote

$$L_1(\rho_\theta, \phi_\omega) = \left\| \mathcal{H}_1(\rho_\theta, \phi_\omega) \right\|_{L^2(E_1)}^2 + \left\| \phi_\omega(T, x) - \phi(T, x) \right\|_{L^2(\Omega)}^2, \quad (6)$$

---

**Algorithm 1** New-Method

---

**Require:**  $H$  Hamiltonian,  $\nu$  diffusion parameter,  $g$  terminal cost.

**Require:** Initialize neural networks  $N_{\omega_0}$  and  $N_{\theta_0}$

**Train**

**for**  $n=0,1,2,\dots,K-2$  **do**

Sample batch  $\{(t_{b_1}, x_{b_1})\}_{b_1=1}^{B_1}$  from  $E_1$ , and  $\{x_{s_1}\}_{s_1=1}^{S_1}$  from  $\Omega$

$$\mathbb{L}^{(HJB)} \leftarrow \frac{1}{B_1} \sum_{b_1=1}^{B_1} \left| \partial_t \phi_{\omega_n}(t_{b_1}, x_{b_1}) + \nu \Delta \phi_{\omega_n}(t_{b_1}, x_{b_1}) - H(x_{b_1}, \rho_{\theta_n}(t_{b_1}, x_{b_1}), \nabla \phi_{\omega_n}(t_{b_1}, x_{b_1})) \right|^2.$$

$$\mathbb{L}_{cond}^{(HJB)} \leftarrow \frac{1}{S_1} \sum_{s_1=1}^{S_1} \left| \phi_{\omega_n}(T, x_{s_1}) - g(x_{s_1}, \rho_{\theta_n}(T, x_{s_1})) \right|^2.$$

Backpropagate  $\text{LOSS}_{total}^{(HJB)}$  to  $\omega_{n+1}$ ,  $\theta_{n+1}$  weights.

Sample batch  $\{(t_{b_2}, x_{b_2})\}_{b_2=1}^{B_2}$  from  $E_2$ , and  $\{x_{s_2}\}_{s_2=1}^{S_2}$  from  $\Omega$ .

$$\mathbb{L}^{(FP)} \leftarrow \frac{1}{B_2} \sum_{b_2=1}^{B_2} \left| \partial_t \rho_{\theta_{n+1}}(t_{b_2}, x_{b_2}) - \nu \Delta \rho_{\theta_{n+1}}(t_{b_2}, x_{b_2}) - \text{div}(\nabla_p H(x_{b_2}, \rho_{\theta_{n+1}}(t_{b_2}, x_{b_2}), \nabla \phi_{\omega_{n+1}}(t_{b_2}, x_{b_2})) \times \rho_{\theta_{n+1}}(t_{b_2}, x_{b_2})) \right|^2.$$

$$\mathbb{L}_{cond}^{(FP)} \leftarrow \frac{1}{S_2} \sum_{s_2=1}^{S_2} \left| \rho_{\theta_{n+1}}(0, x_{s_2}) - \rho_0(x_{s_2}) \right|^2.$$

Backpropagate  $\text{LOSS}_{total}^{(FP)}$  to  $\omega_{n+2}$   $\theta_{n+2}$  weights.

**return**  $\theta_K, \omega_K$

---

where

$$\mathcal{H}_1(\rho_\theta, \phi_\omega) = \partial_t \phi_\omega(t, x) + \nu \Delta \phi_\omega(t, x) - H(x, \rho_\theta(t, x), \nabla \phi_\omega(t, x)).$$

$$L_2(\rho_\theta, \phi_\omega) = \left\| \mathcal{H}_2(\rho_\theta, \phi_\omega) \right\|_{L^2(E_2)}^2 + \left\| \rho_\theta(0, x) - \rho_0(x) \right\|_{L^2(\Omega)}^2, \quad (7)$$

and

$$\mathcal{H}_2(\rho_\theta, \phi_\omega) = \partial_t \rho_\theta(t, x) - \nu \Delta \rho_\theta(t, x) - \text{div}(\rho_\theta(t, x) \nabla_p H(x, \rho_\theta(t, x), \nabla \phi_\omega(t, x))).$$

Denote  $\|f(x)\|_{L^2(E)} = (\int_E |f(x)|^2 d\mu(x))^{\frac{1}{2}}$  the norm on  $L^2$  and  $\mu$  is a positive probability density on  $E$ . The aim of our approach is to identify a set of

parameters  $\theta$  and  $\omega$  such that the functions  $\rho_\theta(x, t)$  and  $\phi_\omega(x, t)$  minimizes the error  $L_1(\rho_\theta, \phi_\omega)$  and  $L_2(\rho_\theta, \phi_\omega)$ . If  $L_1(\rho_\theta, \phi_\omega) = 0$  and  $L_2(\rho_\theta, \phi_\omega) = 0$ , then  $\rho_\theta(t, x)$  and  $\phi_\omega(t, x)$  are solutions to (1). To prove the convergence of the neural networks, we use the results [26] on the universal approximation of functions and their derivatives. Define the class of neural networks with a single hidden layer and  $n$  hidden units,

$$\mathcal{N}^n(\sigma) = \left\{ \Phi(t, x) : \mathbb{R}^{1+d} \mapsto \mathbb{R} : \Phi(t, x) = \sum_{i=1}^n \beta_i \sigma \left( \alpha_{1,i} t + \sum_{j=1}^d \alpha_{j,i} x_j + c_j \right) \right\},$$

Where

$$\theta = (\beta_1, \dots, \beta_n, \alpha_{1,1}, \dots, \alpha_{d,n}, c_1, c_1, \dots, c_n) \in \mathbb{R}^{2n+n(1+d)},$$

the vector of the parameter to be learned. The set of all functions implemented by such a network with a single hidden layer and  $n$  hidden units is

$$\mathcal{N}(\sigma) = \bigcup_{n \geq 1} \mathcal{N}^n(\sigma), \quad (8)$$

We consider  $E$  a compact subset of  $\mathbb{R}^{d+1}$ , from [26, Th 3]. we know that if  $\sigma \in \mathcal{C}^2(\mathbb{R}^{d+1})$  is non constant and bounded, then  $\mathcal{N}(\sigma)$  is uniformly 2-dense on  $E$ . This means by [26, Th 2] that for all  $u \in \mathcal{C}^{1,2}([0, T] \times \mathbb{R}^d)$  and  $\epsilon > 0$ , there is  $f_\theta \in \mathcal{N}(\sigma)$  such that:

$$\sup_{(t,x) \in E} |\partial_t u(t, x) - \partial_t f_\theta(t, x)| + \max_{|a| \leq 2} \sup_{(t,x) \in E} |\partial_x^{(a)} u(t, x) - \partial_x^{(a)} f_\theta(t, x)| < \epsilon. \quad (9)$$

To prove the convergence of our algorithm, we make the following assumptions,

- **(H1):**  $E_1, E_2$  are compacts and consider the measures  $\mu_1, \mu_2, \mu_3$ , and  $\mu_4$  whose support is contained in  $E_1, \Omega, E_2$ , and  $\Omega$  respectively.
- **(H2):** System (1) has a unique solution  $(\phi, \rho) \in \mathcal{X} \times \mathcal{X}$  such that:

$$\mathcal{X} = \left\{ u(t, x) \in \mathcal{C}([0, T] \times \Omega) \cap \mathcal{C}^{1+\eta/2, 2+\eta}([0, T] \times \Omega) \right. \\ \left. \text{with } \eta \in (0, 1) \text{ and that } \sup_{(t,x) \in [0, T] \times \Omega} \sum_{k=1}^2 |\nabla_x^{(k)} u(t, x)| < \infty \right\}.$$

- **(H3):**  $H, \nabla_p H, \nabla_{pp} H, \nabla_{\rho\rho} H$  are locally Lipschitz continuous in  $(\rho, p)$  with Lipschitz constant that can have at most polynomial growth in  $\rho$  and  $p$ , uniformly with respect to  $t, x$ .

**Remark 3.1.** *It is important to note that the nonlinear term of  $L_2$  can be simplified as follows,*

$$\begin{aligned} \operatorname{div}(\rho \nabla_p H(x, \rho, \nabla \phi)) &= \nabla_p H(x, \rho, \nabla \phi) \nabla \rho + \nabla_{p\rho} H(x, \rho, \nabla \phi) \nabla \rho \cdot \rho \\ &\quad + \sum_{i,j} \nabla_{p_i p_j} H(x, \rho, \nabla \phi) (\partial_{x_j x_i} \phi) \rho. \end{aligned}$$

**Theorem 3.1.** *Let consider  $\mathcal{N}(\sigma)$  where  $\sigma$  is  $\mathcal{C}^2(\mathbb{R}^{d+1})$ , non constant and bounded. Suppose **(H1)**, **(H2)**, **(H3)** hold. Then for every  $\epsilon_1, \epsilon_2 > 0$ , there exists two positives constant  $C_1, C_2 > 0$  and there exists two functions  $(\rho_\theta, \phi_\omega) \in \mathcal{N}(\sigma) \times \mathcal{N}(\sigma)$ , such that,*

$$L_i(\rho_\theta, \phi_\omega) \leq C_i(\epsilon_1 + \epsilon_2), \quad \text{for } i = \{1, 2\}.$$

The proof of this theorem is in Appendix A.

Now we have  $L_1(\rho_\theta^n, \phi_\omega^n) \mapsto 0$ , and  $L_2(\rho_\theta^n, \phi_\omega^n) \mapsto 0$  as  $n \mapsto \infty$  but it does not necessarily imply that  $(\rho_\theta^n, \phi_\omega^n) \mapsto (\rho, \omega)$  is the unique solution.

We now prove, under stronger conditions, the convergence of the neural network,  $(\rho_\theta^n, \phi_\omega^n)$  to the solution  $(\rho, \phi)$  of the system 1 as  $n \rightarrow \infty$ .

To avoid some difficulties, we add homogeneous boundary conditions that assume the solution is vanishing on the boundary. The MFG system (1) writes

$$\left\{ \begin{array}{l} -\partial_t \phi - \nu \operatorname{div}(a_1(\nabla \phi)) + \gamma(\rho, \nabla \phi) = 0, \text{ in } \Omega_T, \\ \partial_t \rho - \nu \operatorname{div}(a_2(\nabla \rho)) - \operatorname{div}(a_3(\rho, \nabla \phi)) = 0, \text{ in } \Omega_T, \\ \rho(0, x) = \rho_0(x), \quad \phi(T, x) = g(x, \rho(T, x)), \text{ in } \Omega, \\ \rho(t, x) = \phi(t, x) = 0, \text{ in } \Gamma, \end{array} \right. \quad (10)$$

where,  $\Omega_T = (0, T) \times \Omega$ ,  $\Gamma = (0, T) \times \partial\Omega$  and

$$\begin{aligned} a_1(t, x, \nabla \phi) &= \nabla \phi, \\ a_2(t, x, \nabla \rho) &= \nabla \rho, \\ a_3(t, x, \rho, \nabla \phi) &= \rho \nabla_p H(x, \rho, \nabla \phi), \\ \gamma(t, x, \rho, \nabla \phi) &= H(x, \rho, \nabla \phi), \end{aligned}$$

$a_1 : \Omega_T \times \mathbb{R}^N \rightarrow \mathbb{R}^N$ ,  $a_2 : \Omega_T \times \mathbb{R}^N \times \mathbb{R}^N \rightarrow \mathbb{R}^N$ ,  $a_3 : \Omega_T \times \mathbb{R} \times \mathbb{R}^N \rightarrow \mathbb{R}^N$  and  $\gamma : \Omega_T \times \mathbb{R} \times \mathbb{R}^N \rightarrow \mathbb{R}$  are Caratheodory functions.

Then we introduce the approximate problem of the system (10) as

$$\begin{cases} -\partial_t \phi_\omega^n - \nu \operatorname{div} (a_1(\nabla \phi_\omega^n)) + \gamma(\rho_\theta^n, \nabla \phi_\omega^n) = 0, & \text{in } \Omega_T, \\ \partial_t \rho_\theta^n - \nu \operatorname{div} (a_2(\nabla \rho_\theta^n)) - \operatorname{div} (a_3(\rho_\theta^n, \nabla \phi_\omega^n)) = 0, & \text{in } \Omega_T, \\ \rho_\theta^n(0, x) = \rho_0(x), \quad \phi_\omega^n(T, x) = g(x, \rho_\theta^n(T, x)), & \text{in } \Omega, \\ \rho_\theta^n(t, x) = \phi_\omega^n(t, x) = 0. & \text{in } \Gamma, \end{cases} \quad (11)$$

Let us first introduce some definitions.

Let  $r \geq 1$ . In the sequel we denote by  $L^r(0, T; W_0^{1,r}(\Omega))$  the set of functions  $u$  such that  $u \in L^r(\Omega_T)$ ,  $u(t, \cdot) \in W_0^{1,r}(\Omega)$ . The space  $L^r(0, T; W_0^{1,r}(\Omega))$  is equipped with the norm

$$\|u\|_{L^r(0,T;W_0^{1,r}(\Omega))} := \left( \int_0^T \int_\Omega |\nabla u(x, t)|^r dx dt \right)^{\frac{1}{r}},$$

is a Banach space. For  $s, r \geq 1$ , the space  $V_0^{s,r}(\Omega_T) := L^\infty(0, T; L^s(\Omega)) \cap L^r(0, T; W_0^{1,r}(\Omega))$  endowed with the norm

$$\|\varphi\|_{V_0^{s,r}(\Omega_T)} := \operatorname{ess\,sup}_{0 \leq t \leq T} \|\varphi(\cdot, t)\|_{L^s(\Omega)} + \|\varphi\|_{L^r(0,T;W_0^{1,r}(\Omega))},$$

is also a Banach space.

For this convergence, we make the following set of assumptions,

- **(H4):** There is a constant  $\mu > 0$  and positive functions  $\kappa(t, x), \lambda(t, x)$  such that for all  $(t, x) \in \Omega_T$ , we have

$$\|a_3(t, x, \rho, p)\| \leq \mu(\kappa(t, x) + \|p\|), \quad \text{and } |\gamma(t, x, \rho, p)| \leq \lambda(t, x)\|p\|,$$

with  $\kappa \in L^2(\Omega_T)$ ,  $\lambda \in L^{d+2}(\Omega_T)$ .

- **(H5):**  $a_3(t, x, \rho, p)$  and  $\gamma(t, x, \rho, p)$  are Lipschitz continuous in  $(t, x, \rho, p) \in \Omega_T \times \mathbb{R} \times \mathbb{R}^d$  uniformly on compacts of the form  $\{(t, x) \in \bar{\Omega}_T, |\rho| \leq C, |p| \leq C\}$ .
- **(H6):** There is a positive constant  $\alpha > 0$  such that

$$a_3(t, x, \rho, p)p \geq \alpha|p|^2.$$

- **(H7):** For every  $n \in \mathbb{N}$ ,  $\rho_\theta^n, \phi_\omega^n \in \mathcal{C}^{1,2}(\bar{\Omega}_T)$ . In addition,  $(\rho_\theta^n)_{n \in \mathbb{N}}, (\phi_\omega^n)_{n \in \mathbb{N}} \in L^2(\Omega_T)$ .

**Theorem 3.2.** *Under previous assumptions (H4)-(H7), if we assume that (10) has a unique bounded solution  $(\phi, \rho) \in V_0^{2,2} \times V_0^{2,2}$ , then  $(\phi_\omega^n, \rho_\theta^n)$  converge to  $(\phi, \rho)$  strongly in  $L^p(\Omega_T) \times L^p(\Omega_T)$  for every  $p < 2$ .*

The proof of this theorem is in Appendix B. Related Works

#### 4. Related Works

**GANs:** Generative adversarial networks, or GANs, are a class of machine learning introduced in 2014 [27] that have been successful in generating images and processing data [28, 29, 30]. In recent years, there has been increasing interest in using GANs for financial modeling as well [31]. GANs consist of two neural networks, a generator network, and a discriminator network, that work against each other in order to generate samples from a specific distribution. As described in various sources [27, 32, 33], the goal is to reach equilibrium for the following problem,

$$\min_G \max_D \left\{ \mathbb{E}_{x \sim P_{data}(x)} [\log(D(x))] + \mathbb{E}_{z \sim P_g(z)} [\log(1 - D(G(z)))] \right\}, \quad (12)$$

where  $P_{data}(x)$  is the original data and  $P_g(z)$  is the noise data. In (12), the goal is to minimize the generator's output (G) and maximize the discriminator's output (D). This is achieved by comparing the probability of the original data  $P_{data}(x)$  being correctly identified by the discriminator D with the probability of the generated data G produced by the generator using noise data  $P_g(z)$  being incorrectly identified as real by the discriminator  $1 - D(G(z))$ . Essentially, the discriminator is trying to accurately distinguish between real and fake data, while the generator is attempting to create fake data that can deceive the discriminator.

**APAC-Net:** In [17], the authors present a method (APAC-Net) based on GANs for solving high-dimensional MFGs in the stochastic case. They use of the Hopf formula in density space to reformulate the MFGs as a saddle-point problem given by,

$$\inf_{\rho(x,t)} \sup_{\phi(x,t)} \left\{ \mathbb{E}_{z \sim P(z), t \sim Unif[0,T]} [\partial_t \phi(\rho(t, z), t) + \nu \Delta \phi(\rho(t, z), t) - H(\rho(t, z), \nabla \phi)] + \mathbb{E}_{z \sim P(z)} \phi(0, \rho(0, z)) - \mathbb{E}_{x \sim \rho_T} \phi(T, x) \right\}, \quad (13)$$

where

$$H(x, p) = \inf_v \{-p \cdot v + L(x, v)\}.$$

In this case, we have a connection between the GANs and MFGs, since (13) allows them to reach the Kantorovich-Rubenstein dual formulation of Wasserstein GANs [33] given by,

$$\min_G \max_D \{ \mathbb{E}_{x \sim P_{data}(x)} [(D(x))] - \mathbb{E}_{z \sim P_g(z)} [(D(G(z)))] \}, \quad (14)$$

$$s.t. \quad \|\nabla D\| \leq 1.$$

Finally, we can use an algorithm similar to GANs to solve the problems of MFGs. Unfortunately, we notice that the Hamiltonian in this situation has a separable structure. Due to this, we cannot solve the MFG-LWR system (to be detailed in section 5.3). In general, we cannot solve the MFGs problems, where its Hamiltonian is non-separable, since we cannot reformulate MFGs as 13.

**MFGANs:** In [18, 17], the connection between GANs and MFGs is demonstrated by the fact that equation (13) allows them to both reach the Kantorovich-Rubenstein dual formulation of Wasserstein GANs, as described in reference [33]. This is shown in equation (12), which can be solved using an algorithm similar to those used for GANs. However, it is not possible to solve MFGs problems with non-separable Hamiltonians, as they cannot be reformulated as in equation (13). This is because the Hamiltonian in these cases has a separable structure, which prevents the solution of the MFG-LWR system (to be discussed in section 5.3).

**DGM-MFG:** In [34], section 4 discusses the adaptation of the DGM algorithm to solve mean field games, referred to as DGM-MFG. This method is highly versatile and can effectively solve a wide range of partial differential equations due to its lack of reliance on the specific structure of the problem. Our own work is similar to DGM-MFG in that we also utilize neural networks to approximate unknown functions and adjust parameters to minimize a loss function based on the PDE residual, as seen in [34] and [18]. However, our approach, referred to as New-Method, differs in the way it is trained. Instead of using the sum of PDE residuals as the loss function and SGD for optimization, we define a separate loss function for each equation and use ADAM for training, following the approach in [18]. This modification allows

for faster and more accurate convergence.

**Policy iteration Method:** To the best of our knowledge, [22] was the first to successfully solve systems of mean field game partial differential equations with non-separable Hamiltonians. They proposed two algorithms based on policy iteration, which involve iteratively updating the population distribution, value function, and control. These algorithms only require the solution of two decoupled, linear PDEs at each iteration due to the fixed control. This approach reduces the complexity of the equations, but it is limited to low-dimensional problems due to the computationally intensive nature of the method. In contrast, our method utilizes neural networks to solve the HJB and FP equations at each iteration, allowing for updates to the population distribution and value function in each equation without the limitations of [22].

## 5. Numerical Experiments

To evaluate the effectiveness of the proposed algorithm [1], we use the example provided in [17], as it has an explicitly defined solution structure that allows for easy numerical comparison. We compare the performance of New-Method, APAC-Net’s MFGAN, and DGM-MFG on the same data to assess their reliability. Additionally, we apply New-Method to the traffic flow problem [19], which is characterized by its non-separable Hamiltonian [20], to determine its ability to solve this type of problem in a stochastic case.

### 5.1. Analytic Comparison

We test our method by comparing it to a simple example of the analytic solution used to test the effectiveness of Apac-Net [17]. For the sake of simplicity, we take the spatial domain  $\Omega = [-2, 2]^d$ , the final time  $T = 1$ , and without congestion ( $\gamma = 0$ ). For

$$\begin{aligned} H_0(x, p) &= \frac{\|p\|^2}{2} - \beta \frac{\|x\|^2}{2}, & f_0(x, \rho) &= \gamma \ln(\rho), \\ g(x) &= \alpha \frac{\|x\|^2}{2} - (\nu d \alpha + \gamma \frac{d}{2} \ln \frac{\alpha}{2\pi\nu}), \end{aligned} \tag{15}$$

and  $\nu = \beta = 1$ , where

$$\alpha = \frac{-\gamma + \sqrt{\gamma^2 + 4\nu^2\beta}}{2\nu} = 1.$$

The corresponding MFG system is:

$$\begin{cases} -\partial_t \phi - \Delta \phi + \frac{\|\nabla \phi\|^2}{2} - \frac{\|x\|^2}{2} = 0, \\ \partial_t \rho - \Delta \rho - \operatorname{div}(\rho \nabla \phi) = 0, \\ \rho(0, x) = \left(\frac{1}{2\pi}\right)^{\frac{d}{2}} e^{-\frac{\|x\|^2}{2}}, \\ \phi(T, x) = \frac{x^2}{2} - d, \end{cases} \quad (16)$$

and the explicit formula is given by

$$\begin{aligned} \phi(t, x) &= \frac{\|x\|^2}{2} - d.t, \\ \rho(t, x) &= \left(\frac{1}{2\pi}\right)^{\frac{d}{2}} e^{-\frac{\|x\|^2}{2}}. \end{aligned} \quad (17)$$

**Test 1:** We consider the system of PDEs [16] in one dimension ( $d = 1$ ). To obtain results, we run Algorithm [1] for  $5 \cdot 10^3$  iterations, using a minibatch of 50 samples at each iteration. The neural networks employed have three hidden layers with 100 neurons each, and utilize the Softplus activation function for  $N_\omega$  and the Tanh activation function for  $N_\theta$ . Both networks use ADAM with a learning rate of  $10^{-4}$  and a weight decay of  $10^{-3}$ . We employ ResNet as the architecture of the neural networks, with a skip connection weight of 0.5. The numerical results are shown in Figure 2, which compares the approximate solutions obtained by New-Method to the exact solutions at different time states.

To evaluate the performance of New-Method, we compute the relative error between the model predictions and the exact solutions on a  $100 \times 100$  grid within the domain  $[0, 1] \times [-2, 2]$ . Additionally, we plot the HJB and FP residual loss, as defined in Algorithm [1], to monitor the convergence of our method (see Figure 3).

**Test 2:** In this experiment, we use a single hidden layer with varying numbers of hidden units (nU) for both neural networks. As previously shown in section 2, the number of hidden units can affect the convergence of the model. To verify this, we repeat the previous test using the same hyperparameters and a single hidden layer but with different numbers of hidden units. The relative error between the model predictions and the exact solutions is then calculated on a  $100 \times 100$  grid within the domain  $[0, 1] \times [-2, 2]$ , as shown in Figure 4.

**Test 3:** We solve the MFG system [16] for dimensions 2, 50, and 100. Figure 5 shows the residuals of the HJB and FP equations over  $5 \cdot 10^4$  iterations. A minibatch of 1024, 512, and 128 samples were used for  $d=100$ ,  $d=50$ , and  $d=2$ , respectively. The neural networks had three hidden layers

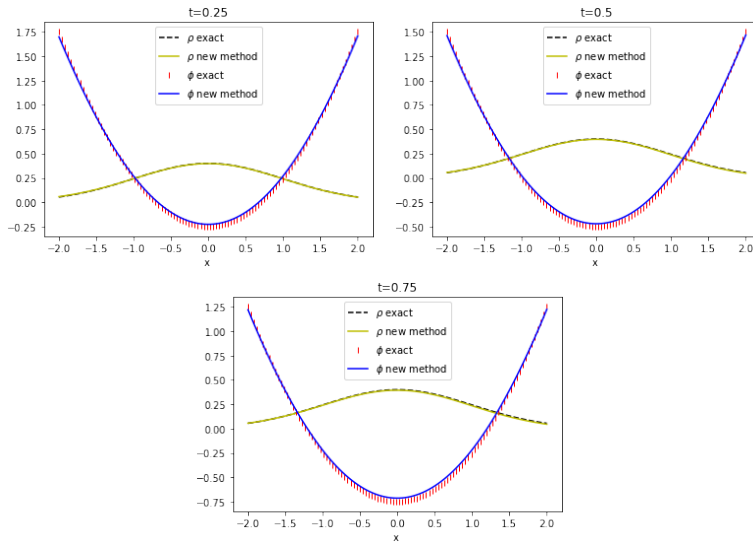


Figure 2: The exact solution and prediction calculated by New-Method in dimension one at  $t=(0.25, 0.5, 0.75)$ .

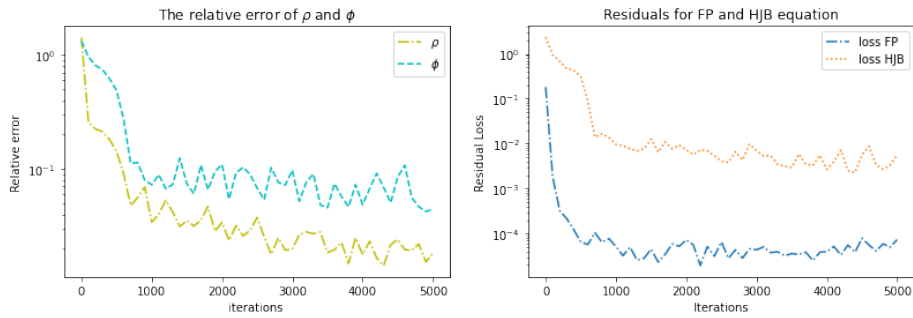


Figure 3: The relative error for  $\rho, \phi$  for the figure on the left. On the right, the HJB, FP Loss.

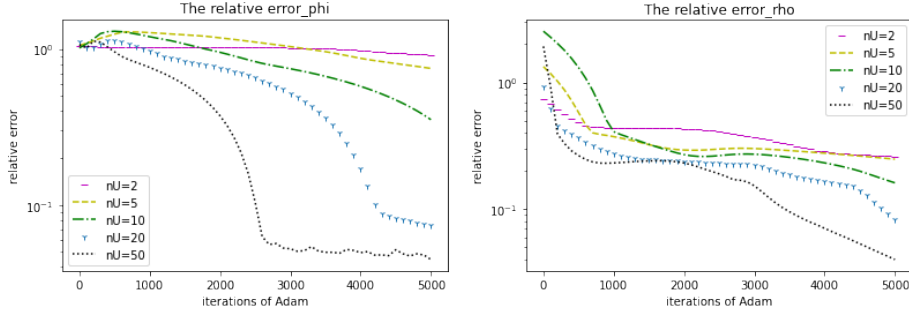


Figure 4: The relative error for  $\rho$ ,  $\phi$  in 1-dimension for  $nU=(2, 5, 10, 20, 50)$ .

with 100 neurons each and utilized the Softplus activation function for  $N_\omega$  and the Tanh activation function for  $N_\theta$ . Both networks used ADAM with a learning rate of  $10^{-4}$ , weight decay of  $10^{-3}$ , and employed ResNet as their architecture with a skip connection weight of 0.5. The results were obtained by recording the residuals every 100 iterations and using a rolling average over 5 points to smooth out the curves.

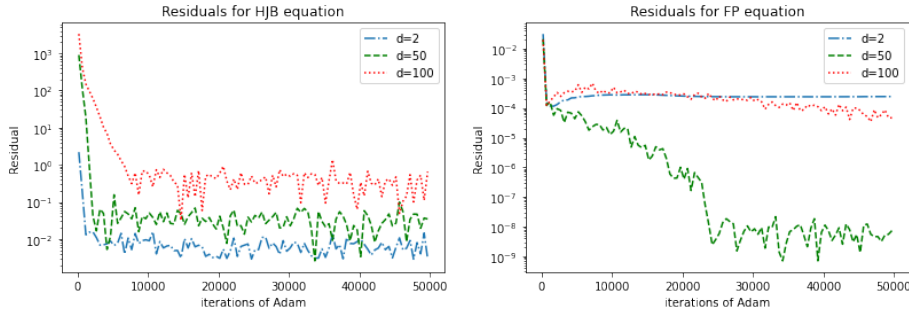


Figure 5: The loss HJB and FP equation for  $d=(2,10,100)$

**Test 4:** In this test, we use the same setup as before, but with a single layer of 100 neurons instead of multiple layers. We keep all other neural network hyperparameters unchanged. This test is meant to demonstrate that a single layer can perform better than multiple layers, even when the dimension increases, as seen in section 2. Figure 6 shows improved results compared to the previous test, even with few iterations, which allows for faster computation times.

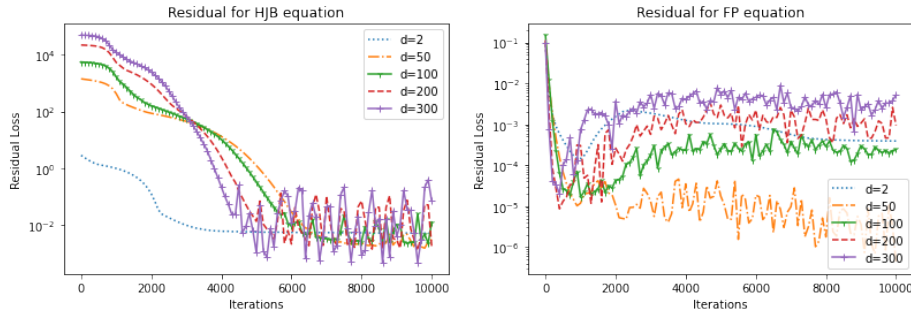


Figure 6: The loss HJB and FP equation with a minibatch of 128, 512, and 1024 samples for  $d=2$ ,  $d=50$ , and  $d=(100,200,300)$ , respectively.

### 5.2. Comparison

In previous sections, we introduced and discussed four methods for solving MFGs: APAC-Net, MFGAN, DGM-MFG, and New-Method. Here, we compare these approaches to assess their performance. For APAC-Net, it is only possible to compare the cost values  $\phi$  due to the unavailability of the density function. In APAC-Net, the generator neural network represents  $\rho$ , which generates the distribution. In order to compare the results, we need to use kernel density estimation to transform the distribution into a density, which is only an estimate. We use the simple example from the analytic solution with  $d = 1$  and  $T = 1$  for this comparison. The two neural networks in this comparison have three hidden layers with 100 neurons each, and utilize ResNet as their architecture with a skip connection weight of 0.5. They also use the Softplus activation function for  $N_\omega$  and the Tanh activation function for  $N_\theta$ . For training APAC-Net, MFGAN, and New-Method, we use ADAM with a learning rate of  $10^{-4}$  and a weight decay of  $10^{-3}$  for both networks. For training DGM-MFG, we use SGD initialized with a value of  $10^{-3}$  and a weight decay of  $10^{-3}$  for both networks.

We run the four algorithms for  $5 \cdot 10^3$  iterations, using a minibatch of 50 samples at each iteration. The relative error between the model predictions and the exact solutions is then calculated on a  $100 \times 100$  grid within the domain  $[0, 1] \times [-2, 2]$ , as shown in Figure 7.

### 5.3. Application (Traffic Flow):

In a study published in [1], the authors focused on the longitudinal speed control of autonomous vehicles. They developed a mathematical model called

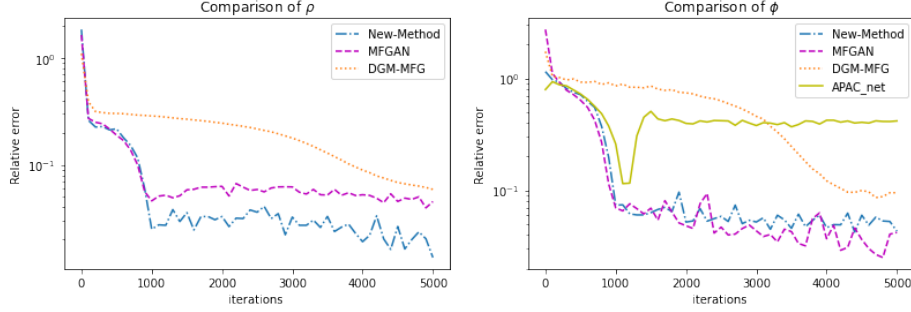


Figure 7: comparison between APAC-Net, MFGAN, DGM-MFG, and New-Method.

a Mean Field Game (MFG) to solve a traffic flow problem for autonomous vehicles and demonstrated that the traditional Lighthill-Whitham-Richards (LWR) model can be used as a solution to the MFG-LWR model described by the following system of equations:

$$MFG - LWR \begin{cases} V_t + U(\rho)V_x - \frac{1}{2}V_x^2 = 0, \\ \rho_t + (\rho u)_x = 0, \\ u = U(\rho) - V_x, \\ V_T = g(\cdot, \rho_T), \quad \rho(\cdot, 0) = \rho_0. \end{cases} \quad (18)$$

Here,  $\rho$ ,  $V$ , and  $u$  represent the density, optimal cost, and speed function, respectively, and the Greenshields density-speed relation is given by  $U(\rho) = u_{max}(1 - \rho/\rho_{jam})$ , where  $\rho_{jam}$  is the jam density and  $u_{max}$  is the maximum speed. By setting  $\rho_{jam} = 1$  and  $u_{max} = 1$ , the authors generalized the MFG-LWR model to include a viscosity term  $\mu > 0$ , resulting in the following system:

$$MFG - LWR \begin{cases} V_t + \nu\Delta V - H(x, p, \rho) = 0, \\ \rho_t - \nu\Delta\rho - \text{div}(\nabla_p H(x, p, \rho)\rho) = 0, \\ V_T = g(\cdot, \rho_T), \quad \rho(\cdot, 0) = \rho_0. \end{cases} \quad (19)$$

In this model,  $\rho$  and  $V$  represent the density and optimal cost function, respectively, and  $H$  is the Hamiltonian with a non-separable structure given by

$$H(x, p, \rho) = \frac{1}{2}\|p\|^2 - (1 - \rho)p, \quad \text{with } p = V_x, \quad (20)$$

where  $p = V_x$ . The authors solved the system in (19) using the Newton Iteration method for the deterministic case ( $\nu = 0$ ) with a numerical

method that considers only a finite number of discretization points to reduce computational complexity. In this work, we propose a new method using a neural network to approximate the unknown and solve the problem in the stochastic case, while also avoiding the computational complexity of the previous method. To evaluate the performance of the new method, we consider the traffic flow problem defined by the MFG-LWR model in 19 with a non-separable Hamiltonian in (20) on the spatial domain  $\Omega = [0, 1]$  with dimension  $d = 1$  and final time  $T = 1$ . The terminal cost  $g$  is set to zero and the initial density  $\rho_0$  is given by a Gaussian distribution,  $\rho_0(x) = 0.2 - 0.6 \exp\left(\frac{-1}{2} \left(\frac{x-0.5}{0.1}\right)^2\right)$ . The aim is to investigate the performance of the new method, called the "New-Method," in solving this traffic flow problem.

The corresponding MFG system is,

$$\begin{cases} V_t + \nu \Delta V - \frac{1}{2} \|V_x\|^2 + (1 - \rho)V_x = 0 \\ \rho_t - \nu \Delta \rho - \operatorname{div}((V_x - (1 - \rho))\rho) = 0 \\ \rho(x, 0) = 0.2 - 0.6 \exp\left(\frac{-1}{2} \left(\frac{x-0.5}{0.1}\right)^2\right), \\ \phi(x, T) = 0. \end{cases} \quad (21)$$

We study the deterministic case ( $\nu = 0$ ) and stochastic case ( $\nu = 0.5$ ). We represent the unknown solutions by two neural networks  $N_\omega$  and  $N_\theta$ , which have a single hidden layer of 50 neurons. We use the ResNet architecture with a skip connection weight of 0.5. We employ ADAM with learning rate  $4 \times 10^{-4}$  for  $N_\omega$  and  $5 \times 10^{-4}$  for  $N_\theta$  and weight decay of  $10^{-4}$  for both networks, batch size 100, in both cases  $\nu = 0$  and  $\nu = 0.5$  we use the activation function Softmax and Relu for  $N_\omega$  and  $N_\theta$  respectively. In Figure 8 we plot over different times the density function, the optimal cost, and the speed which is calculated according to the density and the optimal cost [1] by the following formula,

$$u = u_{max}(1 - \rho/\rho_{jam}) - V_x$$

where, we take the jam density  $\rho_{jam} = 1$  and the maximum speed  $u_{max} = 1$  and  $10^4$  iterations.

++ In Figure (9), we plot the HJB, FP residual loss for  $\nu = 0$  and  $\nu = 0.5$ , which helps us monitor the convergence of our method. Unfortunately, we do not have the exact solution to compute the error. To validate the results of Figure (8), we use the fundamental traffic flow diagram, an essential tool to comprehend classic traffic flow models. Precisely, this is a graphic that

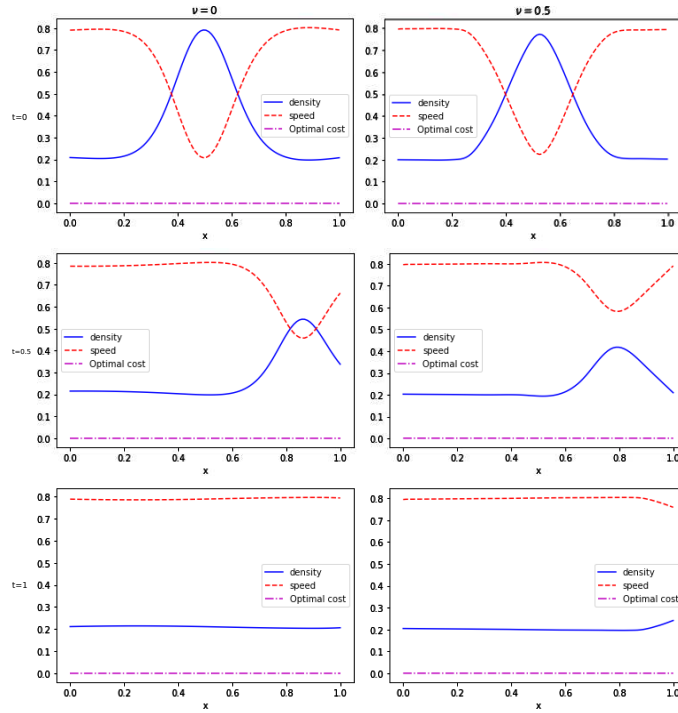


Figure 8: The solution of the problem MFG-LWR by New-Method for ( $\nu = 0$ ) and ( $\nu = 0.5$ ) at  $t=(0,0.5,1)$ .

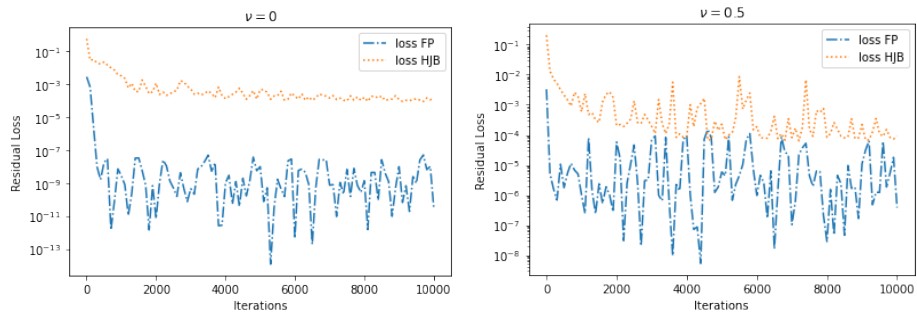


Figure 9: The loss HJB and FP equation for ( $\nu = 0$ ) and ( $\nu = 0.5$ ).

displays a link between road traffic flux (vehicles/hour) and the traffic density (vehicles/km) [35, 36, 37]. We can find this diagram numerically [1] such as its function  $q$  is given by,

$$q(t, x) = \rho(t, x)u(t, x).$$

Figure (10) shows the fundamental diagram of our results.

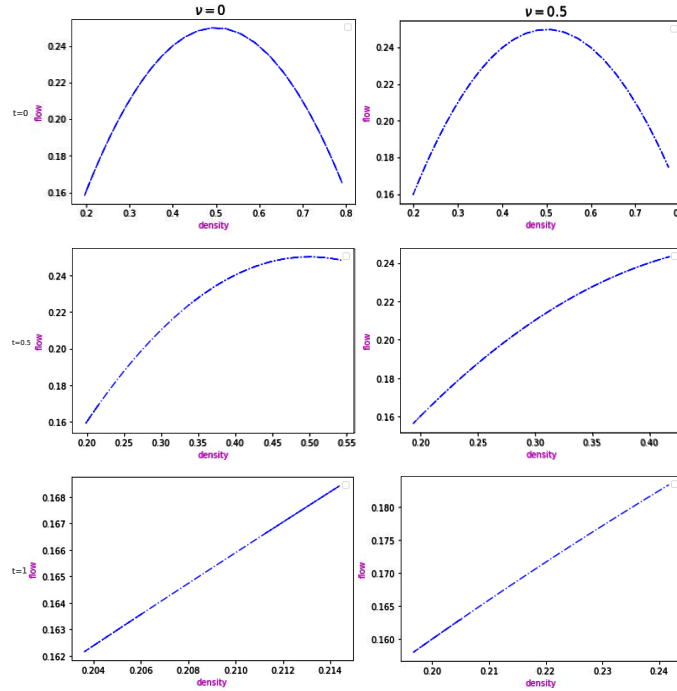


Figure 10: Fundamental diagram for  $\nu = (0, 0.5)$  at  $t = (0, 0.5, 1)$ .

## 6. Conclusion

- We present a new method based on the deep galerkin method (DGM) for solving high-dimensional stochastic mean field games (MFGs). The key idea of our algorithm is to approximate the unknown solutions by two neural networks that were simultaneously trained to satisfy each equation of the MFGs system and forward-backward conditions.
- Consequently, our method shows better results even in a small number of iterations because of its learning mechanism. Moreover, it shows the

potential of up to 300 dimensions with a single layer, which gives more speed to our method.

- we proved that as the number of hidden units increases, the neural networks converge to the MFG solution.
- Comparison with the previous methods shows the efficiency of our approach even with multilayer neural networks.
- Test on traffic flow problem in the deterministic case gives results similar to the newton iteration method, showing that it can solve this problem in the stochastic case.

To address the issue of high dimensions in the problem, we used a neural network but found that it took a significant amount of time. While our approach has helped to reduce the time required, it is still not fast enough. Therefore, we are seeking an alternative to neural networks in future research to improve efficiency.

### Appendix A. Proof of Theorem 3.1.

Denote  $\mathcal{N}(\sigma)$  the space of all functions implemented by such a network with a single hidden layer and  $n$  hidden units, where  $\sigma$  in  $\mathcal{C}^2(\mathbb{R}^{d+1})$  non-constant, and bonded. By **(H1)** we have that for all  $\rho, \phi \in \mathcal{C}^{1,2}([0, T] \times \mathbb{R}^d)$  and  $\varepsilon_1, \varepsilon_2 > 0$ , There is  $\rho_\theta, \phi_\omega \in \mathcal{N}(\sigma)$  such That,

$$\begin{aligned} & \sup_{(t,x) \in E_1} |\partial_t \phi(t, x) - \partial_t \phi_\omega(t, x)| \\ & + \max_{|a| \leq 2} \sup_{(t,x) \in E_1} |\partial_x^{(a)} \phi(t, x) - \partial_x^{(a)} \phi_\omega(t, x)| < \epsilon_1 \end{aligned} \tag{A.1}$$

$$\begin{aligned} & \sup_{(t,x) \in E_2} |\partial_t \rho(t, x) - \partial_t \rho_\theta(t, x)| \\ & + \max_{|a| \leq 2} \sup_{(t,x) \in E_2} |\partial_x^{(a)} \rho(t, x) - \partial_x^{(a)} \rho_\theta(t, x)| < \epsilon_2 \end{aligned} \tag{A.2}$$

From **(H3)** we have that  $(\rho, p) \mapsto H(x, \rho, p)$  is locally Lipschitz continuous in  $(\rho, p)$ , with Lipschitz constant that can have at most polynomial growth in  $\rho$  and  $p$ , uniformly with respect to  $t, x$ . This means that

$$\begin{aligned} |H(x, \rho, p) - H(x, \gamma, s)| & \leq \left( |\rho|^{q_1/2} + |p|^{q_2/2} + |\gamma|^{q_3/2} + |s|^{q_4/2} \right) \\ & \quad \times (|\rho - \gamma| + |p - s|). \end{aligned}$$

with some constants  $0 \leq q_1, q_2, q_3, q_4 < \infty$ . As a result, we get using Hölder inequality with exponents  $r_1, r_2$ ,

$$\begin{aligned}
& \int_{E_1} |H(x, \rho_\theta, \nabla_x \phi_\omega) - H(x, \rho, \nabla \phi)|^2 d\mu_1(t, x) \\
& \leq \int_{E_1} (|\rho_\theta(t, x)|^{q_1} + |\nabla \phi_\omega(t, x)|^{q_2} + |\rho(t, x)|^{q_3} + |\nabla \phi(t, x)|^{q_4}) \\
& \quad \times (|\rho_\theta(t, x) - \rho(t, x)|^2 + |\nabla \phi_\omega(t, x) - \nabla \phi(t, x)|^2) d\mu_1(t, x) \\
& \leq \left( \int_{E_1} (|\rho_\theta(t, x)|^{q_1} + |\nabla \phi_\omega(t, x)|^{q_2} + |\rho(t, x)|^{q_3} + |\nabla \phi(t, x)|^{q_4})^{r_1} d\mu_1(t, x) \right)^{1/r_1} \\
& \quad \times \left( \int_{E_1} (|\rho_\theta(t, x) - \rho(t, x)|^2 + |\nabla \phi_\omega(t, x) - \nabla \phi(t, x)|^2)^{r_2} d\mu_1(t, x) \right)^{1/r_2} \\
& \leq C_1 \left( \int_{E_1} (|\rho_\theta(t, x) - \rho(t, x)|^{q_1} + |\nabla \phi_\omega(t, x) - \nabla \phi(t, x)|^{q_2} \right. \\
& \quad \left. + |\rho(t, x)|^{q_1 \vee q_3} + |\nabla \phi(t, x)|^{q_2 \vee q_4})^{r_1} d\mu_1(t, x) \right)^{1/r_1} \\
& \quad \times \left( \int_{E_1} (|\rho_\theta(t, x) - \rho(t, x)|^2 + |\nabla \phi_\omega(t, x) - \nabla \phi(t, x)|^2)^{r_2} d\mu_1(t, x) \right)^{1/r_2} \\
& \leq C_1 \left( \epsilon_1^{q_1} + \epsilon_2^{q_2} + \sup_{E_1} |\rho|^{q_1 \vee q_3} + \sup_{E_1} |\nabla \phi|^{q_2 \vee q_4} \right) (\epsilon_1^2 + \epsilon_2^2) \\
& \leq C_1 (\epsilon_1^2 + \epsilon_2^2),
\end{aligned}$$

where the constant  $C_1 < \infty$  may change from line to line and  $q_i \vee q_j = \max\{q_i, q_j\}$ . In the two last steps we used A.1, A.2 and **(H2)**. We recall that,

$$\mathcal{H}_1(\rho_\theta, \phi_\omega) = \partial_t \phi_\omega(t, x) + \nu \Delta \phi_\omega(t, x) - H(x, \rho_\theta(t, x), \nabla \phi_\omega(t, x)).$$

Note that  $\mathcal{H}_1(\rho, \phi) = 0$  for  $\rho, \theta$  that solves the system of PDEs,

$$\begin{aligned}
L_1(\rho_\theta, \phi_\omega) &= \left\| \mathcal{H}_1(\rho_\theta, \phi_\omega) \right\|_{L^2(E_1)}^2 + \left\| \phi_\omega(T, x) - \phi(T, x) \right\|_{L^2(\Omega)}^2 \\
&= \left\| \mathcal{H}_1(\rho_\theta, \phi_\omega) - \mathcal{H}_1(\rho, \phi) \right\|_{L^2(E_1)}^2 + \left\| \phi_\omega(x, T) - g(x, \rho_\theta(x, T)) \right\|_{L^2(\Omega)}^2 \\
&\leq \int_{E_1} |\partial_t \phi_\omega(t, x) - \partial_t \phi(t, x)|^2 d\mu_1(t, x) \\
&\quad + |\nu| \int_{E_1} |\Delta \phi_\omega(t, x) - \Delta \phi(t, x)|^2 d\mu_1(t, x) \\
&\quad + \int_{E_1} |H(x, \rho_\theta, \nabla \phi_\omega) - H(x, \rho, \nabla \phi)|^2 d\mu_1(t, x) \\
&\quad + \int_{\Omega} |\phi_\omega(T, x) - \phi(T, x)|^2 d\mu_2(t, x) \\
&\leq C_1(\epsilon_1^2 + \epsilon_2^2)
\end{aligned}$$

for an appropriate constant  $C_1 < \infty$ . In the last step, we use A.1, A.2 and the previous result.

For  $L_2$  we use remark 3.1 to simplified the nonlinear term,

$$\operatorname{div}(\rho \nabla_p H(x, \rho, \nabla \phi)) = \alpha_1(x, \rho, \nabla \phi) + \alpha_2(x, \rho, \nabla \phi) + \alpha_3(x, \rho, \nabla \phi),$$

where,

$$\begin{aligned}
\alpha_1(x, \rho, \nabla \phi) &= \nabla_p H(x, \rho, \nabla \phi) \nabla \rho, \\
\alpha_2(x, \rho, \nabla \phi) &= \nabla_{p\rho} H(x, \rho, \nabla \phi) \nabla \rho \cdot \rho, \\
\alpha_3(x, \rho, \nabla \phi) &= \sum_{i,j} \nabla_{p_i p_j} H(x, \rho, \nabla \phi) (\partial_{x_j x_i} \phi) \rho.
\end{aligned}$$

In addition, from **(H3)** we have also  $\nabla_p H(x, \rho, p)$ ,  $\nabla_{p\rho} H(x, \rho, p)$ , and  $\nabla_{pp} H(x, \rho, p)$  are locally Lipschitz continuous in  $(\rho, p)$ . Then, we have after an application of Holder inequality, for some constant  $C_2 < \infty$  that may change from line

to line,

$$\begin{aligned}
& \int_{E_2} |\alpha_1(x, \rho_\theta, \nabla \phi_\omega) - \alpha_1(x, \rho, \nabla \phi)|^2 d\mu_3(t, x) \\
&= \int_{E_2} |\nabla_{p_\omega} H(x, \rho_\theta, \nabla \phi_\omega) \nabla \rho_\theta - \nabla_p H(x, \rho, \nabla \phi) \nabla \rho|^2 d\mu_3(t, x) \\
&\leq \int_{E_2} \left| \left( \nabla_{p_\omega} H(x, \rho_\theta, \nabla \phi_\omega) - \nabla_p H(x, \rho, \nabla \phi) \right) \nabla \rho \right|^2 d\mu_3(t, x) \\
&\quad + \int_{E_2} \left| \nabla_{p_\omega} H(x, \rho_\theta, \nabla \phi_\omega) (\nabla \rho_\theta - \nabla \rho) \right|^2 d\mu_3(t, x) \\
&\leq C_2 \left( \int_{E_2} \left| \nabla_{p_\omega} H(x, \rho_\theta, \nabla \phi_\omega) - \nabla_p H(x, \rho, \nabla \phi) \right|^{2r_1} d\mu_3(t, x) \right)^{1/r_1} \\
&\quad \times \left( \int_{E_2} |\nabla \rho|^{2r_2} d\mu_3(t, x) \right)^{1/r_2} + C_2 \left( \int_{E_2} \left| \nabla_{p_\omega} H(x, \rho_\theta, \phi_\omega) \right|^{2s_1} d\mu_3(t, x) \right)^{1/s_1} \\
&\quad \times \left( \int_{E_2} |\nabla \rho_\theta - \nabla \rho|^{2s_2} d\mu_3(t, x) \right)^{1/s_2} \\
&\leq C_2 \left( \int_{E_2} |\nabla \rho|^{2r_2} d\mu_3(t, x) \right)^{1/r_2} \\
&\quad \times \left( \int_{E_2} (|\rho_\theta(t, x) - \rho(t, x)|^{q_1} + |\nabla \phi_\omega(t, x) - \nabla \phi(t, x)|^{q_2} \right. \\
&\quad \left. + |\rho(t, x)|^{q_1 \vee q_3} + |\nabla \phi(t, x)|^{q_2 \vee q_4})^{v_1 r_1} d\mu_3(t, x) \right)^{1/v_1 r_1} \\
&\quad \times \left( \int_{E_2} (|\rho_\theta(t, x) - \rho(t, x)|^2 + |\nabla_x \phi_\omega(t, x) - \nabla_x \phi(t, x)|^2)^{v_2 r_2} d\mu_3(t, x) \right)^{1/v_2 r_2} \\
&\quad + C_2 \left( \int_{E_2} \left| \nabla_{p_\omega} H(x, \rho_\theta, \phi_\omega) \right|^{2s_1} d\mu_3(t, x) \right)^{1/s_1} \times \left( \int_{E_2} |\nabla \rho_\theta - \nabla \rho|^{2s_2} d\mu_3(t, x) \right)^{1/s_2} \\
&\leq C_2(\epsilon_1^2 + \epsilon_2^2)
\end{aligned}$$

where in the last steps, we followed the computations previously. We do same for  $\alpha_2(x, \rho, \nabla \phi)$  and  $\alpha_3(x, \rho, \nabla \phi)$ , we obtain for a  $C_2 < \infty$ ,

$$\begin{aligned}
& \int_{E_2} \left| \operatorname{div}(\rho_\theta \nabla_{p_\omega} H(x, \rho_\theta, \nabla \phi_\omega)) - \operatorname{div}(\rho \nabla_p H(x, \rho, \nabla \phi)) \right|^2 d\mu_3(t, x) \\
&\leq C_2(\epsilon_1^2 + \epsilon_2^2).
\end{aligned}$$

We recall that,

$$\mathcal{H}_2(\rho_\theta, \phi_\omega) = \partial_t \rho_\theta(t, x) - \nu \Delta \rho_\theta(t, x) - \operatorname{div}(\rho_\theta(t, x) \nabla_p H(x, \rho_\theta(t, x), \nabla \phi_\omega(t, x)))$$

Note that  $\mathcal{H}_2(\rho, \phi) = 0$  for  $\rho, \theta$  that solves the system of PDEs, then we have,

$$\begin{aligned} L_2(\rho_\theta, \phi_\omega) &= \left\| \mathcal{H}_2(\rho_\theta, \phi_\omega) \right\|_{L^2(E_2)}^2 + \left\| \rho_\theta(0, x) - \rho_0(x) \right\|_{L^2(\Omega)}^2 \\ &= \left\| \mathcal{H}_2(\rho_\theta, \phi_\omega) - \mathcal{H}_2(\rho, \phi) \right\|_{L^2(E_2)}^2 + \left\| \rho_\theta(0, x) - \rho_0(x) \right\|_{L^2(\Omega)}^2 \\ &\leq \int_{E_2} |\partial_t \rho_\theta(t, x) - \partial_t \rho(t, x)|^2 d\mu_3(t, x) \\ &\quad + |\nu| \int_{E_2} |\Delta \rho_\theta(t, x) - \Delta \rho(t, x)|^2 d\mu_3(t, x) \\ &\quad + \int_{E_2} \left| \operatorname{div}(\rho_\theta \nabla_{p_\omega} H(x, \rho_\theta, \nabla \phi_\omega)) - \operatorname{div}(\rho \nabla_p H(x, \rho, \nabla \phi)) \right|^2 d\mu_3(t, x) \\ &\quad + \int_{\Omega} |\rho_\theta(0, x) - \rho_0(x)|^2 d\mu_4(t, x) \\ &\leq C_2(\epsilon_1^2 + \epsilon_2^2) \end{aligned}$$

for an appropriate constant  $C_2 < \infty$ . The proof of theorem 3.1 is complete after rescaling  $\epsilon_1$  and  $\epsilon_2$

## Appendix B. Proof of Theorem 3.2.

We follow the method used in [23] for a single PDE. (See also section 4 in [38] for a coupled system). Let us denote the solution of problem 11 by  $(\hat{\rho}_\theta^n, \hat{\phi}_\omega^n) \in V = V_0^{2,2} \times V_0^{2,2}$ . Due to Conditions  $(H_4) - (H_6)$  and by using lemma 1.4 [39] on each equation then, there exist,  $C_1, C_2$  such that:

$$\|\hat{\rho}_\theta^n\|_{V_0^{2,2}} \leq C_1$$

$$\|\hat{\phi}_\omega^n\|_{V_0^{2,2}} \leq C_2$$

These applies and gives that the both sequence  $\{\hat{\rho}_\theta^n\}_{n \in \mathbf{N}}, \{\hat{\phi}_\omega^n\}_{n \in \mathbf{N}}$  are uniformly bounded with respect to  $n$  in at least  $V$ . These uniform energy bounds

imply the existence of two subsequences, (still denoted in the same way)  $\{\hat{\rho}_\theta^n\}_{n \in \mathbb{N}}$ ,  $\{\hat{\phi}_\omega^n\}_{n \in \mathbb{N}}$  and two functions  $\rho$ ,  $\phi$  in  $L^2(0, T; W_0^{1,2}(\Omega))$  such that,

$$\hat{\rho}_\theta^n \rightarrow \rho \text{ weakly in } L^2(0, T; W_0^{1,2}(\Omega))$$

$$\hat{\phi}_\omega^n \rightarrow \phi \text{ weakly in } L^2(0, T; W_0^{1,2}(\Omega))$$

Next let us set  $q = 1 + \frac{d}{d+4} \in (1, 2)$  and note that for conjugates,  $r_1, r_2 > 1$  such that  $1/r_1 + 1/r_2 = 1$

$$\begin{aligned} \int_{\Omega_T} \left| \gamma \left( t, x, \hat{\rho}_\theta^n, \nabla \hat{\phi}_\omega^n \right) \right|^q &\leq \int_{\Omega_T} |\lambda|^q \left| \nabla \hat{\phi}_\omega^n \right|^q \\ &\leq \left( \int_{\Omega_T} |\lambda|^{r_1 q} \right)^{1/r_1} \left( \int_{\Omega_T} \left| \nabla \hat{\phi}_\omega^n \right|^{r_2 q} \right)^{1/r_2} \end{aligned}$$

Let us choose  $r_2 = 2/q > 1$ . Then we calculate  $r_1 = \frac{r_2}{r_2-1} = \frac{2}{2-q}$ . Hence, we have that  $r_1 q = d + 2$ . Recalling the assumption  $\lambda \in L^{d+2}(\Omega_T)$  and the uniform bound on the  $\nabla \hat{\phi}_\omega^n$  we subsequently obtain that for  $q = 1 + \frac{d}{d+4}$ , there is a constant  $C < \infty$  such that

$$\int_{\Omega_T} \left| \gamma \left( t, x, \hat{\rho}_\theta^n, \nabla \hat{\phi}_\omega^n \right) \right|^q \leq C$$

On the other hand, it is obvious that  $a_1$  is bounded uniformly then, according to the HJB equation of 11, we have  $\left\{ \partial_t \hat{\phi}_\omega^n \right\}_{n \in \mathbb{N}}$  is bounded uniformly with respect to  $n$  in  $L^2(0, T; W^{-1,2}(\Omega))$ . Then we can extract a subsequence, (still denoted in the same way)  $\left\{ \partial_t \hat{\phi}_\omega^n \right\}_{n \in \mathbb{N}}$  such that

$$\partial_t \hat{\phi}_\omega^n \rightarrow \partial_t \phi \text{ weakly in } L^2(0, T; W^{-1,2}(\Omega))$$

Also, it will be shown that

$$\partial_t \hat{\rho}_\theta^n \rightarrow \partial_t \rho \text{ weakly in } L^2(0, T; W^{-1,2}(\Omega))$$

Since the problem is nonlinear, the weak convergence of  $\hat{\phi}_\omega^n$  and  $\hat{\rho}_\theta^n$  in the space  $L^2(0, T; W_0^{1,2}(\Omega))$  is not enough in order to prove that  $\phi$  and  $\rho$  are a solution of problem 10. To do this, we need the almost everywhere convergence of the gradients for a subsequence of the approximating solutions  $\hat{\phi}_\omega^n$  and  $\hat{\rho}_\theta^n$ .

However, the uniform boundedness of  $\{\hat{\phi}_\omega^n\}_{n \in \mathbf{N}}$  and  $\{\hat{\rho}_\theta^n\}_{n \in \mathbf{N}}$  in  $L^2(0, T; W_0^{1,2}(\Omega))$  and their weak convergence to  $\phi$  and  $\rho$  respectively in that space, allows us to conclude, by using Theorem 3.3 of [40] on each equation, that

$$\nabla \hat{\phi}_\omega^n \rightharpoonup \nabla \phi \text{ almost everywhere in } \Omega_T.$$

$$\nabla \hat{\rho}_\theta^n \rightharpoonup \nabla \rho \text{ almost everywhere in } \Omega_T.$$

Hence, we obtain that  $\{\hat{\phi}_\omega^n\}_{n \in \mathbf{N}}$  and  $\{\hat{\rho}_\theta^n\}_{n \in \mathbf{N}}$  converges respectively to  $\phi$  and  $\rho$  strongly in  $L^p(0, T; W_0^{1,p}(\Omega))$  for every  $p < 2$ . It remains to discuss the convergence of  $\phi_\omega^n - \hat{\phi}_\omega^n$  and  $\rho_\theta^n - \hat{\rho}_\theta^n$  to zero. By last step of proof theorem 7.3 [23] we get  $\{\phi_\omega^n - \hat{\phi}_\omega^n\}_{n \in \mathbf{N}}$  and  $\{\rho_\theta^n - \hat{\rho}_\theta^n\}_{n \in \mathbf{N}}$  goes to zero strongly in  $L^p(\Omega_T)$  for every  $p < 2$ . Finally we conclude the proof of the convergence in  $L^p(\Omega_T)$  for every  $p < 2$

## References

- [1] K. Huang, X. Di, Q. Du, X. Chen, A game-theoretic framework for autonomous vehicles velocity control: Bridging microscopic differential games and macroscopic mean field games, arXiv preprint arXiv:1903.06053 (2019).
- [2] H. Shiri, J. Park, M. Bennis, Massive autonomous uav path planning: A neural network based mean-field game theoretic approach, in: 2019 IEEE Global Communications Conference (GLOBECOM), IEEE, 2019, pp. 1–6.
- [3] P. Cardaliaguet, C.-A. Lehalle, Mean field game of controls and an application to trade crowding, *Mathematics and Financial Economics* 12 (3) (2018) 335–363.
- [4] P. Casgrain, S. Jaimungal, Algorithmic trading in competitive markets with mean field games, *SIAM News* 52 (2) (2019) 1–2.
- [5] Y. Achdou, J. Han, J.-M. Lasry, P.-L. Lions, B. Moll, Income and wealth distribution in macroeconomics: A continuous-time approach, Tech. rep., National Bureau of Economic Research (2017).
- [6] Y. Achdou, F. J. Buera, J.-M. Lasry, P.-L. Lions, B. Moll, Partial differential equation models in macroeconomics, *Philosophical Transactions*

of the Royal Society A: Mathematical, Physical and Engineering Sciences 372 (2028) (2014) 20130397.

- [7] D. A. Gomes, L. Nurbekyan, E. Pimentel, Economic models and mean-field games theory, Publicacoes Matematicas, IMPA, Rio, Brazil (2015).
- [8] A. De Paola, V. Trovato, D. Angeli, G. Strbac, A mean field game approach for distributed control of thermostatic loads acting in simultaneous energy-frequency response markets, IEEE Transactions on Smart Grid 10 (6) (2019) 5987–5999.
- [9] A. C. Kizilkale, R. Salhab, R. P. Malhamé, An integral control formulation of mean field game based large scale coordination of loads in smart grids, Automatica 100 (2019) 312–322.
- [10] D. Gomes, J. Saúde, A mean-field game approach to price formation in electricity markets, arXiv preprint arXiv:1807.07088 (2018).
- [11] J. Han, Q. Li, et al., A mean-field optimal control formulation of deep learning, arXiv preprint arXiv:1807.01083 (2018).
- [12] X. Guo, A. Hu, R. Xu, J. Zhang, Learning mean-field games, arXiv preprint arXiv:1901.09585 (2019).
- [13] Y. Achdou, I. Capuzzo-Dolcetta, Mean field games: numerical methods, SIAM Journal on Numerical Analysis 48 (3) (2010) 1136–1162.
- [14] J.-D. Benamou, G. Carlier, F. Santambrogio, Variational mean field games, in: Active Particles, Volume 1, Springer, 2017, pp. 141–171.
- [15] Y. T. Chow, J. Darbon, S. Osher, W. Yin, Algorithm for overcoming the curse of dimensionality for time-dependent non-convex hamilton–jacobi equations arising from optimal control and differential games problems, Journal of Scientific Computing 73 (2) (2017) 617–643.
- [16] Y. T. Chow, J. Darbon, S. Osher, W. Yin, Algorithm for overcoming the curse of dimensionality for certain non-convex hamilton–jacobi equations, projections and differential games, Annals of Mathematical Sciences and Applications 3 (2) (2018) 369–403.

- [17] A. T. Lin, S. W. Fung, W. Li, L. Nurbekyan, S. J. Osher, Apac-net: Alternating the population and agent control via two neural networks to solve high-dimensional stochastic mean field games, arXiv preprint arXiv:2002.10113 (2020).
- [18] H. Cao, X. Guo, M. Laurière, Connecting gans, mfgs, and ot, arXiv preprint arXiv:2002.04112 (2020).
- [19] J.-M. Lasry, P.-L. Lions, Mean field games, Japanese journal of mathematics 2 (1) (2007) 229–260.
- [20] M. Cirant, L. Nurbekyan, The variational structure and time-periodic solutions for mean-field games systems, arXiv preprint arXiv:1804.08943 (2018).
- [21] Y. T. Chow, W. Li, S. Osher, W. Yin, Algorithm for hamilton–jacobi equations in density space via a generalized hopf formula, Journal of Scientific Computing 80 (2) (2019) 1195–1239.
- [22] M. Laurière, J. Song, Q. Tang, Policy iteration method for time-dependent mean field games systems with non-separable hamiltonians, arXiv preprint arXiv:2110.02552 (2021).
- [23] J. Sirignano, K. Spiliopoulos, Dgm: A deep learning algorithm for solving partial differential equations, Journal of computational physics 375 (2018) 1339–1364.
- [24] M. Raissi, P. Perdikaris, G. E. Karniadakis, Physics informed deep learning (part i): Data-driven solutions of nonlinear partial differential equations, arXiv preprint arXiv:1711.10561 (2017).
- [25] M. Raissi, Deep hidden physics models: Deep learning of nonlinear partial differential equations, The Journal of Machine Learning Research 19 (1) (2018) 932–955.
- [26] K. Hornik, Approximation capabilities of multilayer feedforward networks, Neural networks 4 (2) (1991) 251–257.
- [27] I. Goodfellow, J. Pouget-Abadie, M. Mirza, B. Xu, D. Warde-Farley, S. Ozair, A. Courville, Y. Bengio, Generative adversarial networks, Communications of the ACM 63 (11) (2020) 139–144.

- [28] E. Denton, S. Chintala, A. Szlam, R. Fergus, Deep generative image models using a laplacian pyramid of adversarial networks, arXiv preprint arXiv:1506.05751 (2015).
- [29] S. Reed, Z. Akata, X. Yan, L. Logeswaran, B. Schiele, H. Lee, Generative adversarial text to image synthesis, in: International Conference on Machine Learning, PMLR, 2016, pp. 1060–1069.
- [30] A. Radford, L. Metz, S. Chintala, Unsupervised representation learning with deep convolutional generative adversarial networks, arXiv preprint arXiv:1511.06434 (2015).
- [31] M. Wiese, L. Bai, B. Wood, H. Buehler, Deep hedging: learning to simulate equity option markets, arXiv preprint arXiv:1911.01700 (2019).
- [32] Y. Dukler, W. Li, A. Lin, G. Montúfar, Wasserstein of wasserstein loss for learning generative models, in: International Conference on Machine Learning, PMLR, 2019, pp. 1716–1725.
- [33] C. Villani, Topics in optimal transportation, Vol. 58, American Mathematical Soc., 2021.
- [34] R. Carmona, M. Laurière, Deep learning for mean field games and mean field control with applications to finance, arXiv preprint arXiv:2107.04568 (2021).
- [35] F. Siebel, W. Mauser, On the fundamental diagram of traffic flow, SIAM Journal on Applied Mathematics 66 (4) (2006) 1150–1162.
- [36] N. Geroliminis, C. F. Daganzo, Existence of urban-scale macroscopic fundamental diagrams: Some experimental findings, Transportation Research Part B: Methodological 42 (9) (2008) 759–770.
- [37] M. Keyvan-Ekbatani, A. Kouvelas, I. Papamichail, M. Papageorgiou, Exploiting the fundamental diagram of urban networks for feedback-based gating, Transportation Research Part B: Methodological 46 (10) (2012) 1393–1403.
- [38] F. O. Gallego, M. T. G. Montesinos, Existence of a capacity solution to a coupled nonlinear parabolic–elliptic system, Communications on Pure & Applied Analysis 6 (1) (2007) 23.

- [39] M. M. Porzio, Existence of solutions for some" noncoercive" parabolic equations, *Discrete & Continuous Dynamical Systems* 5 (3) (1999) 553.
- [40] L. Boccardo, A. Dall'Aglio, T. Gallouët, L. Orsina, Nonlinear parabolic equations with measure data, *journal of functional analysis* 147 (1) (1997) 237–258.